Multi-focus Image Fusion using the Local Neighbor Sum of Laplacian in NSCT Domain

Peng Geng*, Zhiwei Gao and Changxia Hu

School of Information Science and Technology, Shijiazhuang Tiedao University, Gengpeng@stdu.edu.cn

Abstract

To suppress the Pseudo-Gibbs phenomena caused by the Contourlet, the Nonsubsampled Pyramids Filter Banks and the Nonsubsampled Directional Filter Banks are combined to construct the nonsubsampled Contourlet transform (NSCT). Hence, The NSCT not only possess the main features of multi-scale, multi-directional and time-frequency localization, but also offer the property of the shift-invariant which is vital to image processing. Firstly, multi-scale decomposition is performed on source images using NSCT to get high-frequency and low-frequency images. Secondly, the Novel Sum-Modified-Laplacian and Local Neighbour Sum of Laplacian are respectively used to select the lowpass coefficient and highpass coefficients to combine fused image. Finally, the inverse nonsubsampled contourlet transform is applied to obtain fused image. Experimental results show the proposed approach outperform the traditional discrete wavelet transform-based and the Contourlet-based image fusion methods.

Keywords: *nonsubsampled Contourlet transform, Sum-Modified-Laplacian, Sum of Laplacian*

1. Introduction

Image fusion is the process extracting and synthesizing information from multiple sources, such as multi-sensor, multi-focus, multi-spectral or multi-frame images, in order to produce a more accurate, more reliable composite result than any single image from multiple different sources. The benefits of image fusion include improved spatial awareness, increased accuracy in target detection and recognition, reduced operator workload and increased system reliability. [1]. Multi-focus image fusion is an important branch of this field. Due to the limited depth-of-focus of optical lenses in camera, it is often not possible to obtain an image that contains all relevant focused objects [2]. One way to overcome this problem is by using the multi-focus image fusion technique, through which several images with different focus points are combined to form a single image with all objects fully focused.

Many fusion techniques and algorithms for pixel-level fusion have been proposed, from the simplest weighted averaging to more advanced pyramidal methods. Recently, several multi-scale geometric analysis (MGA) tools, such as Ridgelet, Curvelet, and Contourlet transform have been developed. The MGA can take full advantage of the geometric regularity of image intrinsic structures and obtain the asymptotic optimal representation. The fusion scheme based on the discrete wavelet transform (DWT) generally produces good results and is computationally efficient.

Unfortunately, the DWT is not shift-invariant, because of the downsamplers used in its calculation [3]. The Contourlet can give the asymptotic optimal representation of contours and has been successfully used in image fusion field [4]. In [4] a novel image fusion method based on Contourlet domain hidden Markov tree models is proposed. However, the Contourlet lack of shift-invariance and results in artifacts along the edges to some extend. In 2006, Cunha, *et al.*, proposed an overcomplete transform, namely, the nonsubsampled contourlet transform [5] (NSCT), which has been successfully used in image denoising and image enhancement. The NSCT inherits the perfect properties of the Contourlet, and meanwhile possesses the shift-invariance. When the NSCT is used into the image fusion field, more information for fusion can be obtained. So, the NSCT is more suitable for image fusion.

In this paper, a new multi-focus image fusion algorithm based on NSCT is put forward in this study. The new modified Sum-Modified-Laplacian (MSML) [6] method is used to select the lowpass coefficients and the Local Neighbor Sum of Laplacian (LNML) rule is applied to fuse the highpass coefficients in this study. The NSCT Coefficients with greater MSML and LNML are selected out to combine fused image when high-frequency and low-frequency NSCT subbands of source images are compared.

2. NSCT

Since it can very well describe the image edge feature, contourlet transform has been widely applied [7]. However, the contourlet transform frequency information is not fully utilized, and the lack of shift-invariance causes Pseudo-Gibbs phenomena in the reconstruction. To suppress the Pseudo-Gibbs phenomena caused by the Contourlet, the Nonsubsampled Pyramids Filter Banks (NSPFB) and the Nonsubsampled Directional Filter Banks (NSDFB) [8] are combined to construct the nonsubsampled contourlet transform (NSCT). The NSCT not only possess the main features of multi-scale, multi-directional and time-frequency localization, but also offer a high degree of directionality and anisotropy, which can easily capture the frequency localization property [9]. Especially, it has shift-invariant which is vital to image processing.

NSPFB is obtained by Laplacian Pyramid has removed the downsamplers and upsamplers for the filters [10]. NSPFB is upsamplers for lowpass filter $H_0(z)$ and highpass filter $H_1(z)$. Then, the low frequency image of up scale is decomposed into high-frequency and low-frequency two parts. The structure chart is illustrated in Figure 1.

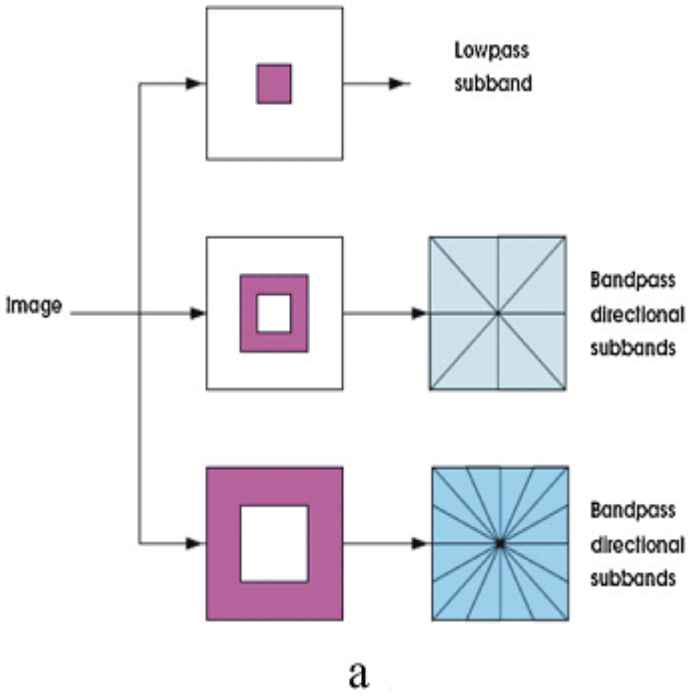

Figure 1. NSFB Structure that Implements the NSCT

The NSP perfect reconstruction conditions as follows:

$$H_0(z)G_0(z) + H_1(z)G_1(z) = 1 \tag{1}$$

Where $H_0(z)$ and $H_1(z)$ respectively express the lowpass decomposition filter and highpass decomposition filter, $G_1(z)$ and $G_1(z)$ respectively express the lowpass reconstruction filter and highpass reconstruction filter [8].

NSDFB is a shift-invariant version of directional filter banks in contourlet transform by eliminating the downsampler and upsamplers [8]. It results in a two-channel directional filter banks that are used iteratively. In a four-channel directional decomposition, the upsampled filters is $U_j(z^D)$, where j=0,1 and the sampling matrix D is selected as quincunx matrix $D = \begin{bmatrix} 1 & -1 \\ 1 & 1 \end{bmatrix} a$. The equivalent filter $U_k(z)$ in each channel, k=0,1,2,3, is decided by Formula (2). The structure chart of NSDFB is illustrated in Figure 2.

$$U_k(z) = U_i(z)U_j(z^D) \tag{2}$$

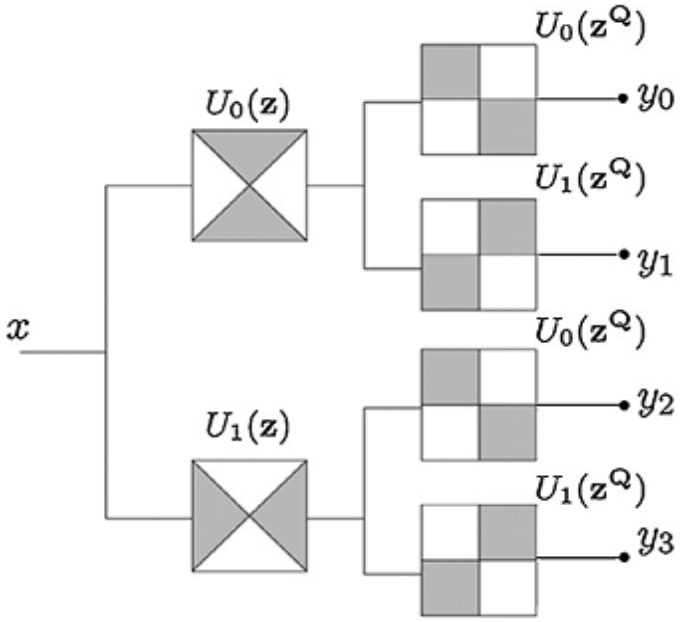

Figure 2. NSDFB Constructed with Two-channel Fan Filter Bank

3. Fusion Rule

3.1. Low Frequency Coefficients Fusion Rule

A focus measure is defined which is a maximum for the best focused image and it generally decreases as the defocus increases. Therefore, in the field of multifocus image fusion, the focused image areas of the source images must produce maximum focus measures; the defocused areas must produce minimum focus measures in contrast. Let I(*m*,*n*) be the gray level intensity of pixel (*m*,*n*).

The ML (Modified Laplacian) takes the absolute values of the second derivatives in the Laplacian to avoid the cancellation of second derivatives in the horizontal and vertical directions that have opposite signs. The ML is defined as follows:

$$\begin{aligned} \mathrm{ML}_{j,l}(\mathrm{m},\mathrm{n}) = &\left|2I_{j,l}(\mathrm{m},\mathrm{n}) - I_{j,l}(m-step,n) - I_{j,l}(m+step,n)\right| \\ &+\left|2I_{j,l}(\mathrm{m},\mathrm{n}) - I_{j,l}(\mathrm{m},\mathrm{n}-step) - I_{j,l}(\mathrm{m},\mathrm{n}+step)\right| \end{aligned} \tag{3}$$

Where the parameters $I_{j,l}(m,n)$ is the coefficient located at (*m*,*n*) in the *j*-th scale and *l*-th direction subband.

In order to accommodate for possible variations in the size of texture elements, Nayar (1994) [11] used a variable spacing (step) between the pixels to compute ML. In this paper 'step' always equals to 1. The focus measure at a point (*m*,*n*) is computed as the SML (sum of the Modified Laplacian) [12-13], in a window around the point:

$$\mathrm{SML}^{l,k}(\mathrm{i},\mathrm{j}) = \sum_{m=-M}^{M}\sum_{n=-N}^{N}[\mathrm{ML}^{l,k}(i+m,\ j+n)]^2 \tag{4}$$

Where the parameters M and N determine the window with size (2M+1)×(2N+1) is used to compute the focus measurement.

In corder to meet human visual system (HVS) requirement, we will take a modified sum-modified-Laplacian (MSML) of the low-frequency to select fusion coefficients in the NSCT lowpass subband. The complete expression of MSML is shown as following.

$$\mathrm{MSML}^{l,k}(\mathrm{i},\mathrm{j}) = \sum_{m=-M}^{M}\sum_{n=-N}^{N}\omega(m,n)[\mathrm{ML}^{l,k}(i+m,\ j+n)]^2 \tag{5}$$

ω is a template which size is relatively small, and must satisfy the normalization rule $\sum\sum\omega(m,n)=1$ .The window size is 3×3. In this paper, the ω is given as:

$$\omega(m,n)=\frac{1}{16}\begin{bmatrix}1 & 2 & 1\\ 2 & 4 & 2\\ 1 & 2 & 1\end{bmatrix}$$

3.2. High Frequency Coefficients Fusion Rule

As the sharpness measure, the modified sum of Laplacian (MSL) of an image can be used as a fusion criterion. It can effectively represent the salient features and sharp edge of image. Larger value of MSL means more high frequency edge information.

$$\begin{aligned}MSL_{j,l}(m,n) = {} & \left|8C_{j,l}(m,n)\right|-\left|4C_{j,l}(m-1,n)\right|-\left|4C_{j,l}(m+1,n)\right|\\ & +\left|8C_{j,l}(m,n)\right|-\left|4C_{j,l}(m,n-1)\right|-\left|4C_{j,l}(m,n+1)\right|\\ & +\left|2C_{j,l}(m,n)\right|-\left|C_{j,l}(m-1,n+1)\right|-\left|C_{j,l}(m+1,n-1)\right|\\ & +\left|2C_{j,l}(m,n)\right|-\left|C_{j,l}(m-1,n-1)\right|-\left|C_{j,l}(m+1,n+1)\right|\end{aligned} \tag{6}$$

To maintain robustness of the algorithm and meet the HVS requirements, a novel local neighborhood sum of Laplacian measurement of the high frequency coefficient (LNML) is used in this paper. The complete expression of LNML is shown in following.

$$\mathrm{L}NML^{l,k}(\mathrm{i},\mathrm{j}) = \sum_{m=-M}^{M}\sum_{n=-N}^{N}\omega(m,n)[\mathrm{MSL}^{l,k}(i+m,\ j+n)]^2 \tag{7}$$

The ω used in the low frequecy coefficient is directly utilized in the high frequency coefficient fusion.

4. Proposed Fusion Algorithm

The image fusion framework based on NSCT is shown in Figure 3. The following steps of image fusion are adopted.

1) Source images A and B are perfect registered

2) Source images A and B are decomposed as $C_{j,k}^{A}(m,n)$ and $C_{j,k}^{B}(m,n)$ by the NSCT, respectively. $C_{j,k}^{A}(m,n)$ and $C_{j,k}^{B}(m,n)$ denote the subband coefficients at the *j*-th scale and the *l*-th direction.

3) Select fusion NSCT coefficients for each high frequency sub-image from A and B according different fusion rules.

4) Finally, apply the inverse NSCT to the fused low and high frequency subband to reconstruct the fused image F.

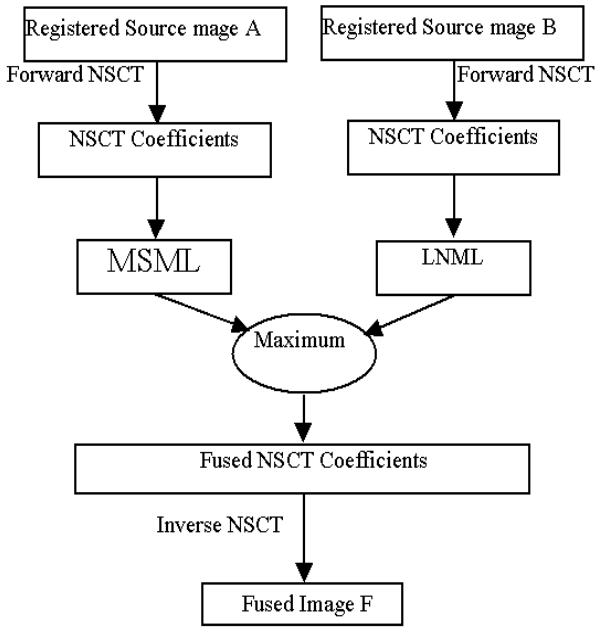

Figure 3. Schematic Diagram of NSCT-based Fusion Algorithm

5. Experiments

Four pairs of multifocus images shown in the Figure 4 are used to perform experiments to show the performance of the proposed approach. For comparison purposes, the fusion is also performed using the DWT-based method, Contourlet-based and the NSCT-based method, in all of which the lowpass subband coefficients and the bandpass subband coefficients are respectively merged by the MSML and LNSL of the transform coefficients, respectively.

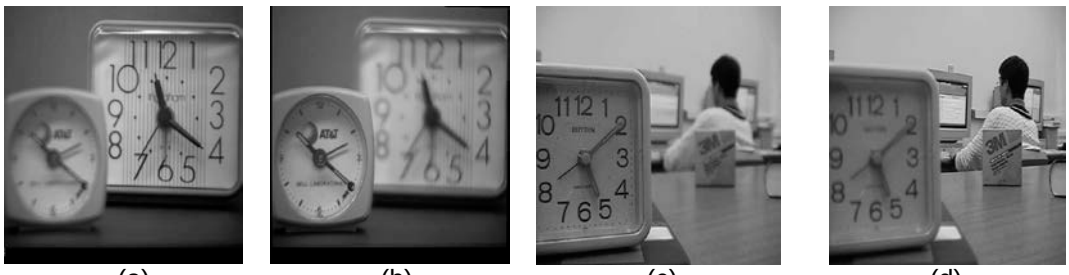

(a) (b) (c) (d)

(e) (f) (g) (h)

Figure 4. Multifocus Images Pairs for Experiment

The ‘db4’ wavelet, together with a decomposition level of 4, is used in the DWT-based and the Contourlet-based methods in which 4 decomposition levels, with 2, 3, 3, 4 directions from coarser scale to finer scale are used. Four decomposition levels, with 4, 8, 8, 16 directions from coarser scale to finer scale, are used in the NSCT methods.

The first experiment is performed on the ‘Clock’ images which have been registered perfectly. Figure 5(a)-(c) illustrates the source images and the fusion results obtained by the above different methods. For a clearer comparison, Figure 5(e)–(f) illustrates the different between the fused image and source image A. The second experiment is performed on the ‘Pepsi’ images, which are also registered perfectly. The fusion results of the image ‘Pepsi’ are shown in Figure 6 (a)–(c) with DWT, Contourlet and NSCT transform by proposed fusion criterion. Figure 6 (e)–(f) shows the difference between fused images by above three methods and the source image A. The third and fourth experiment is performed on the ‘lab’ and ‘disk images. Figure 7 (c)-(e) displays the source images and the fused results by various methods, and Figure 7(g)–(h) shows the different between the fused image and source image A.

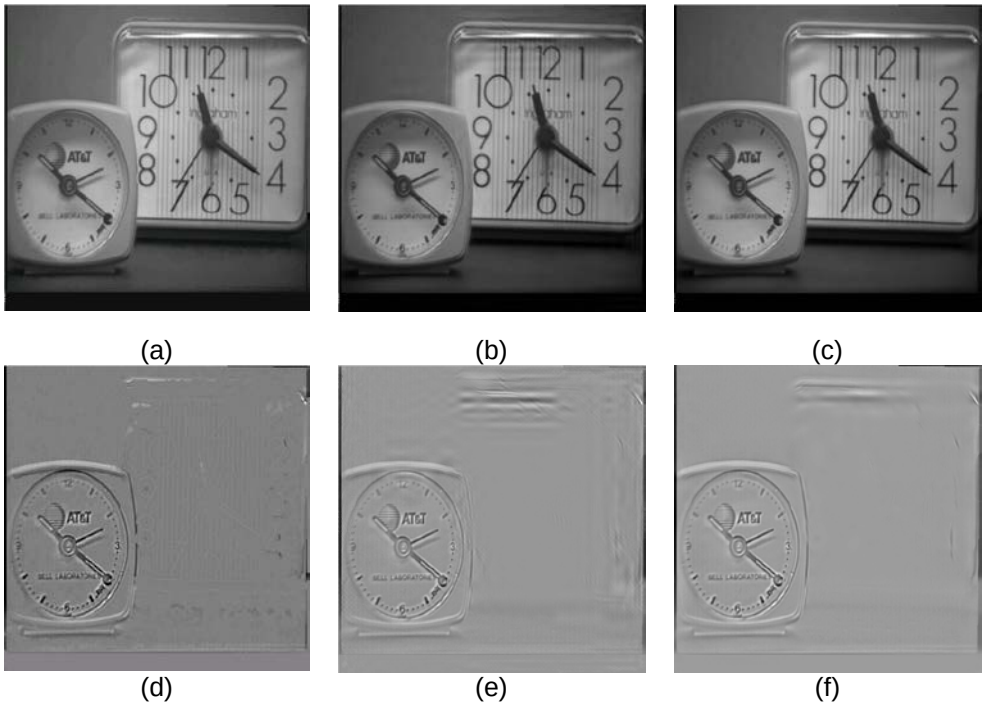

(a) (b) (c)

(d) (e) (f)

Figure 5. The Fusion Results of ‘Clock’ Image by Different Method

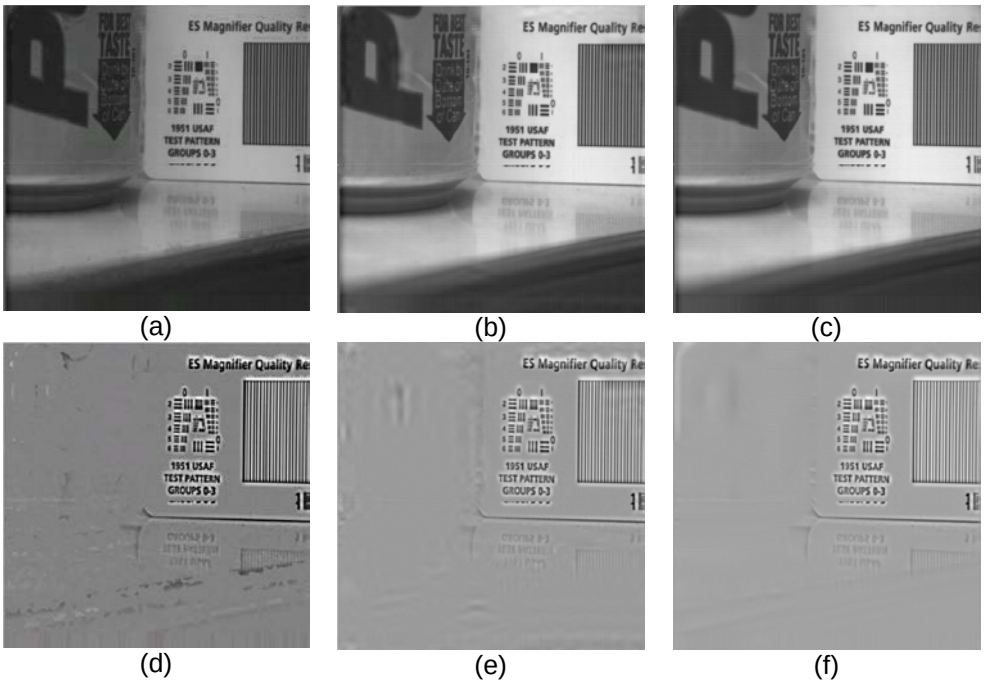

Figure 6. The Fusion Results of 'Pepsi' Image by Different Method

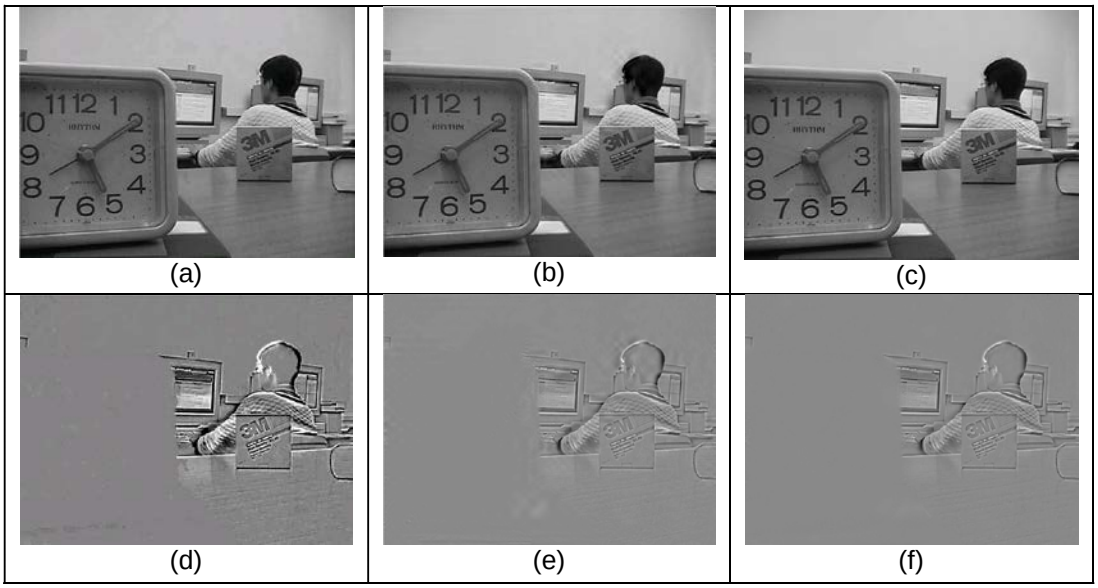

Figure 7. The Fusion Results of 'Lab' Image by Different Method

The fusion result comparisons in Figure 5-Figure 7 show that the fused image attained by our proposed method is the best visual quality. Almost all the useful information of the source images has been transferred to the fused image, and mean time, fewer artifacts are introduced during the fusion process. Evidently, the contrast of the fused image obtained by the DWT-based method is reduced greatly, and many 'artifacts' are introduced in the fused image attained by the DWT-based method.

For further comparison, two objective criteria are used to compare the fusion results. The mutual information (MI) [14] metric proposed by Piella in 2003 and the $Q^{AB/F}$ metric [15], proposed by Xydeas and Petrovic in 2000 are used to evaluate the fusion performance quantitatively in this paper. The MI and $Q^{AB/F}$ values of the different methods in Figure 5-Figure 8, are calculated and shown in Table 1. It can be seen from Table 1 that the MI and $Q^{AB/F}$ value of the proposed method is the largest in the two methods and the MI and $Q^{AB/F}$ value of the DWT method is the smallest. The results presented in this example can demonstrate that our approach can fuse the multi-focus images while retaining much more information than that of the other two methods.

Table 1. Performance of Fusion by Proposed Criterion in Different Transform Coefficients

Images	Criteria	DWT	Contourlet	NSCT
Clock	MI	5.7845	6.6388	**7.1001**
	$Q^{AB/F}$	0.5829	0.6390	**0.6755**
Pepsi	MI	5.9121	6.6225	**7.1989**
	$Q^{AB/F}$	0.6102	0.7343	**0.7588**
Lab	MI	5.9651	6.8365	**7.3873**
	$Q^{AB/F}$	0.6326	0.7033	**0.7285**
Disk	MI	5.7293	6.5188	**6.8136**
	$Q^{AB/F}$	0.5219	0.6541	**0.6885**

6. Conclusion

NSCT has shift-invariant. Because of the Nonsubsampled Pyramids Filter Banks and the Nonsubsampled Directional Filter Banks. The NSCT suppress the Pseudo-Gibbs phenomena caused by the Contourlet transform. Same to the Contourlet transform, NSCT is an image multi-scale geometric analysis tool with many advantages such as multi-scale, localization and multi-direction. Furhtermore, the NSCT is more suitable for image fusion due to the its shift-invariance. Therefore, a new multi-focus image fusion based on MSML and LNSL in the Nonsubsampled Contourlet Transform coefficients is presented. The experimental results show the proposed method outperform the method by DWT and Contourlet transform using MSML and LNSL fusion methods by both visual evaluation and quantities evaluation. The proposed image fusion approach is an effective, efficient and feasible algorithm. However, as for the noised image, the fusion result is affected by the noise. How to suppress the noise is vital to the future work to improve the fusion performance. Another, the improved performance is at the cost of increasing computational complexity and memory during the fusion process. How to reduce the computation complexity is also the future work.

Acknowledgements

Some of the images used in this paper are available le at http: //www.imagefusion.org. This work was supported in part by Natural Science Foundation of Hebei Province under grant 2013210094, the University Science Research Project of Hebei Province under grant 201142. The authors also thank the editors and anonymous reviewers for their valuable suggestions.

References

[1] S. Gabarda and G. Cristóbal, "On the use of a joint spatial-frequency representation for the fusion of multi-focus images", Pattern Recognition Letters, vol. 26, no. 16, **(2005)**, pp. 2572-2578.
[2] Y. Chai, H. Li and Z. Li, "Multifocus image fusion scheme using focused region detection and multiresolution", Optics Communications, vol. 284, no. 19, **(2011)**, pp. 4376-4389.
[3] B. Yang and Z. Jing, "Image fusion using a low-redundancy and nearly shift-invariant discrete wavelet frame", Optical Engineering, vol. 46, no. 10, **(2007)**, pp. 107002-1-107002.
[4] L. Kun, G. Lei and C. Jingsong, "Image Fusion Algorithm Based on Contourlet Domain Hidden Markov Tree Models", ACTA PHOT ON ICA SINICA, vol. 39, no. 8, **(2010)**, pp. 1383-1387.
[5] J. P. Zhou, A. L. da Cunha and M. N. Do, "Nonsubsampled contourlet transform: construction and application in enhancement", Proceedings of IEEE International Conference on Image Processing, Genova, Italy, **(2005)**.
[6] Y. Chai, H. F. Li and M. Y. Guo, "Multifocus image fusion scheme based on features of multiscale products and PCNN in lifting stationary wavelet domain", Optics Communications, vol. 284, no. 5,**(2011)**, pp. 1146-1158.
[7] Z. Hua, Y. Li and J. Li, "Image Nonlinear Enhancement Algorithm based on Nonsubsampled Contourlet Transform", International Journal of Digital Content Technology and its Applications, vol. 5, no. 7, **(2011)**, pp. 43-51.
[8] S. Yang, M. Wang, Y. Xiong Lu, W. Qi and L. Jiao, "Fusion of multiparametric SAR images based on SW-nonsubsampled contourlet and PCNN", Signal Processing. vol. 89, **(2009)**, pp. 2596-2608.
[9] Z. Qiang and G. Bao-long, "Multifocus image fusion using the nonsubsampled contourlet transform", Signal Processing, vol. 89, no. 7, **(2009)**, pp. 1334-1346.
[10] M. Liyong, W. Guoyao and F. Naizhang, "Image fusion of ultrasound tomography based on nonsubsampled contourlet transform and image segmentation", Journal of Convergence Information Technology, vol. 6, no. 10, **(2011)**, pp. 277-283.
[11] S. K. Nayar and Y. Nakagawa, "Shape from focus", IEEE Transactions on Pattern Analysis and Machine Intelligence, vol. 16, no. 8, **(1994)**, pp. 824-831.
[12] Q. Xiaobo, Y. Jingwen and Y. Guide, "Sum-modified-Laplacian-based Multifocus Image Fusion Method in Sharp Frequency Localized Contourlet Transform Domain", Optics and Precision Engineering, vol. 17, no. 5, **(2009)**, pp. 1203-1202.
[13] G. Stanciu Stefan, D. Marin and A. Stanciu George, "Sum-modified-Laplacian Fusion Methods experimented on image stacks of photonic quantum ring laser devices collected by confocal scanning laser microscopy", UPB Scientific Bulletin, Series A: Applied Mathematics and Physics, vol. 73, no. 2, **(2011)**, pp. 139-146.
[14] G. Piella, "A general framework for multiresolution image fusion: from pixels to regions", Information Fusion, vol. 4, no. 4, **(2003)**, pp. 259-280.
[15] C. S. Xydeas and V. Petrovic, "Objective image fusion performance measure", Electronics Letters, vol. 36, no. 4, **(2000)**, pp. 308-309, 17.

Authors

Peng Geng received his Master in the Department of Information Engineering from Shijiazhuang Tiedao University in 2007, and received his B.S.degree from Hebei Normal University in 2001, respectively. He is currently an Associate Professor in the school of information science and technology, Shijiazhuang Tiedao University. His current research interests are focused on image fusion, multiscale analysis, and image denoising.

Zhiwei Gao is an associate professor in the School of information science and technology, ShiJiaZhuang TieDao University. He received his master degree in the Department of computer science from Beijing Jiaotong University 2001. His current research interests are in network security, distributed computing and image denoising.

Hu Changxia received her Master in the Department of Computer and Information Engineering from Shijiazhuang Tiedao University in 2008, and received her B.S. degree from Shijiazhuang Tiedao University in 2001, respectively. She is currently an Associate Professor in the School of Information Science and Technology, Shijiazhuang Tiedao University. Her current research interests are focused on information processing database, WEB application technology.